3-17-2008

An Intense Green/Yellow Dual-Chromatic Calcium Chlorosilicate Phosphor Ca3SiO4Cl2:Eu2+–Mn2+ for Yellow and White LED

Weijia Ding
Sun Yat-sen University, China; South China Agricultural University, China

Jing Wang
Sun Yat-sen University, China

Zongmiao Liu
Sun Yat-sen University, China

Mei Zhang
Sun Yat-sen University, China

Qiang Su
Sun Yat-sen University, China

See next page for additional authors

Publication Information

Ding, Weijia; Wang, Jing; Liu, Zongmiao; Zhang, Mei; Su, Qiang; and Tang, Jinke (2008). "An Intense Green/Yellow Dual-Chromatic Calcium Chlorosilicate Phosphor Ca3SiO4Cl2:Eu2+–Mn2+ for Yellow and White LED." *Journal of The Electrochemical Society* 155.5, J122-J127.

Authors
Weijia Ding, Jing Wang, Zongmiao Liu, Mei Zhang, Qiang Su, and Jinke Tang

Journal of The Electrochemical Society, **155** (5) J122-J127 (2008)
0013-4651/2008/155(5)/J122/6/$23.00 © The Electrochemical Society

An Intense Green/Yellow Dual-Chromatic Calcium Chlorosilicate Phosphor $Ca_3SiO_4Cl_2:Eu^{2+}$–Mn^{2+} for Yellow and White LED

Weijia Ding,[a,b] Jing Wang,[a,z] Zongmiao Liu,[a] Mei Zhang,[a] Qiang Su,[a,z] and Jinke Tang[c]

[a]*Ministry of Education, Laboratory of Bioinorganic and Synthetic Chemistry, State Key Laboratory of Optoelectronic Materials and Technologies, School of Chemistry and Chemical Engineering, Sun Yat-sen University, Guangzhou, Guangdong 510275, China*
[b]*College of Science, South China Agricultural University, Guangzhou 510642, China*
[c]*Department of Physics & Astronomy, University of Wyoming, Laramie, Wyoming 82071, USA*

A series of intense green/yellow phosphors $Ca_3SiO_4Cl_2:Eu^{2+},Mn^{2+}$ was synthesized by a high-temperature solid-state reaction. Their luminescent properties were characterized by means of powder diffuse reflection, photoluminescence excitation and emission spectra, and lifetime and temperature-dependent emission spectra in the temperature range of 10–450 K. The phosphors $Ca_3SiO_4Cl_2:Eu^{2+},Mn^{2+}$ show intense broad absorption bands between 250 and 450 nm, matching well with the near-ultraviolet (380–420 nm) emission band of InGaN-based chips, and exhibit two dominating bands situated at 512 and 570 nm, ascribed to the allowed $5d \rightarrow 4f$ transition of the Eu^{2+} ion and the $^4T_{1g}(^4G) \rightarrow {}^6A_{1g}(^6S)$ transition of the Mn^{2+} ion, respectively. The lifetime of the Eu^{2+} ion decreases with increasing the concentration of the Mn^{2+} ion, strongly supporting an efficient energy transfer from Eu^{2+} to Mn^{2+}. By combining with near-ultraviolet (~395 nm) InGaN chips, intense yellow light-emitting diodes (LEDs) with a much lower ultraviolet light leakage were successfully fabricated based on the $Ca_3SiO_4Cl_2:Eu^{2+},Mn^{2+}$ phosphor, and intense white LEDs were made based on a blend of blue chlorophosphate phosphor and the green/yellow phosphor $Ca_3SiO_4Cl_2:Eu^{2+},Mn^{2+}$. The color coordinate, correlated color temperature T_c, general color-rendering index R_a, and luminous efficiency of the fabricated white LEDs are (0.3281, 0.3071), 6065 K, 84.5, and 11 lm/W, respectively.
 [DOI: 10.1149/1.2890240]

Manuscript submitted October 17, 2007; revised manuscript received February 3, 2008. Available electronically March 17, 2008.

It is well known that the invention of white light-emitting diodes (LEDs) has brought another revolution to the illumination of this century to supersede conventional incandescent or fluorescent lamps because of their excellent properties such as high brightness, reliability, lower power consumption, and long life.[1,2] At present, there are several ways to make the white LEDs.[3,4] One significant scheme is phosphor-converted white LED (pc-wLED) that is further classified into two approaches: blue (440–470 nm) and a near-ultraviolet (n)-UV (390–410 nm) InGaN chip combined with down-converting phosphors. For the blue InGaN chip, the commonly used down-converting phosphor is yellow YAG:Ce^{3+}. However, such white LEDs encounter a low color-rendering index ($R_a < 80$) due to the scarcity of red emission. Besides, the white LED based on the blue InGaN chip encounters a low color reproducibility in the mass manufacture scale. The n-UV LED is considered more stable and efficient with a higher output.[5] In addition, the n-UV LED generally emits at a wavelength shorter than 400 nm, which has little effect on the chromaticity coordinate of pc-wLED, which is generally determined by the visible radiation distribution of phosphor between 380 and 730 nm.[6] Thus, the n-UV pc-wLEDs are expected to have a great application potential in the field of solid-state lighting.

Nowadays, many phosphors have been investigated including orthosilicates, akermanites, aluminates, sulfides, molybdates, and oxynitrides/nitrides. However, they often have some serious drawbacks, for example, low down-converting efficiency, poor chemical stability, and poor high-temperature stability, or harsh synthesis conditions (such as >1700°C high temperature or about a few MPa high pressure).[7-11] Recently, Eu^{2+}-activated chlorosilicates have attracted more attention due to their high luminescent efficiency, low synthesis temperature, and high physical chemistry stability.[8,12-15] In 2005, Liu et al. reported a single green-emitting phosphor based on $Ca_3SiO_4Cl_2:Eu^{2+}$ with a low-temperature phase, and thereafter developed a single yellowish-orange-emitting phosphor based on $Ca_3SiO_4Cl_2:Eu^{2+}$ with a high temperature phase and fabricated a white LED with a low color-rendering index of 73, due to the scarcity of blue and green content in the white emission.[13,15] In this paper, a series of intense dual-chromatic green/yellow emitting phosphors, $Ca_3SiO_4Cl_2:Eu^{2+},Mn^{2+}$, was reported. The highly efficient energy transfer between Eu^{2+} and Mn^{2+} ions was systematically investigated. More importantly, intense yellow LEDs with a low UV leakage and high down-converting efficiency, and white LEDs with a high color-rendering index and high luminous efficiency were successfully fabricated based on $Ca_3SiO_4Cl_2:Eu^{2+},Mn^{2+}$.

Experimental

Synthesis of $Ca_3SiO_4Cl_2:Eu^{2+}$–Mn^{2+}.— Powder samples were synthesized via a solid-state reaction at high temperature. The raw materials were Eu_2O_3 (99.99%), analytical regent grade $CaCO_3$, $CaCl_2$, SiO_2, and $MnCO_3$. The mixtures of corresponding raw materials by a molar ratio of $CaCO_3:SiO_2:CaCl_2 = 2:1:1.1$ and a small amount of Eu_2O_3 and $MnCO_3$ were thoroughly ground with an agate mortar and pestle. They were then put into a corundum crucible and subsequently kept at 1123 K for 4 h in a reducing atmosphere (25% H_2/75% N_2). Finally, as-synthesized samples were slowly cooled to room temperature inside the tube furnace in a nitrogen atmosphere. $Y_3Al_5O_{12}$:0.06Ce was prepared by a solid-state reaction according to Ref. 16.

Characterization of $Ca_3SiO_4Cl_2:Eu^{2+}$–Mn^{2+}.— Powder X-ray diffraction (XRD) was performed on a Rigaku D/max-IIB X-ray diffractometer with Cu $K\alpha_1$ (λ = 1.5405 Å) radiation. The diffuse reflection spectra of as-synthesized samples were measured on a Cary 5000 UV-Vis-NIR spectrophotometer (Varian Inc.) equipped with a double out-of-plane Littrow monochrometer, using $BaSO_4$ as a standard reference in the measurements. The photoluminescence (PL) excitation and emission spectra were measured on a Fluorolog-3 spectrofluorometer (Jobin Yvon Inc./Specx) equipped with a 450 W Xe lamp, double-excitation monochromators, and single-emission monochromator. The room-temperature lifetime measurement and temperature-dependent emission properties of as-synthesized samples in the temperature range of 10–450 K were determined on an FLS920-combined time resolved and steady-state fluorescence spectrometer (Edinburgh Instruments) equipped with the closed-cycle helium cryostats (Advance Inc.).

[z] E-mail: ceswj@mail.sysu.edu.cn; suqiang@mail.sysu.edu.cn

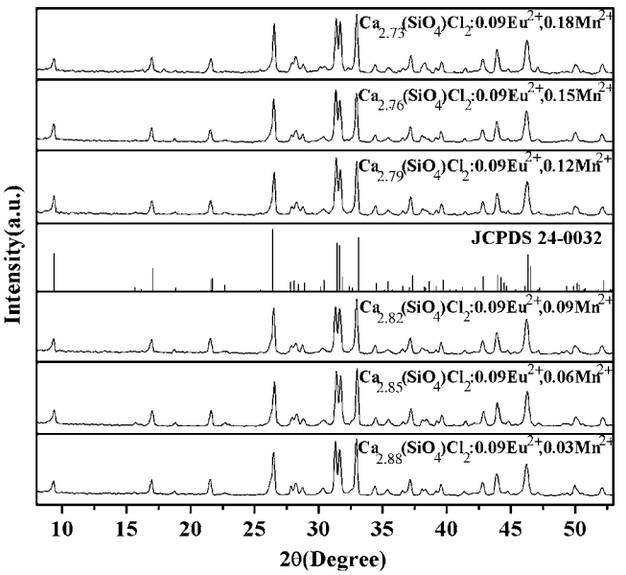

Figure 1. Powder XRD patterns of $Ca_3(SiO_4)Cl_2$ (JCPDS 24–0032) and $Ca_3(SiO_4)Cl_2$:0.09Eu^{2+},xMn^{2+} (x = 0.03, 0.06, 0.09, 0.12, 0.15, 0.18).

Characterization of yellow and white LEDs.— The yellow and white LEDs were fabricated by combining InGaN-based ultraviolet LEDs (Cree Inc., C395-MB290, 12 mW, λ_{em} = 395 nm) and as-synthesized phosphors. Their optical properties were evaluated by an LED-1100 spectral/goniometric analyzer (Labsphere Inc.) under a direct current of 20 mA at room temperature.

Results and Discussion

Photoluminescence properties of $Ca_3SiO_4Cl_2$:Eu^{2+}–Mn^{2+}.— The body colors of the as-synthesized samples doped without and with Eu^{2+} or Eu^{2+}–Mn^{2+} ions were white, green, and yellow. It was reported that $Ca_3(SiO_4)Cl_2$ had a monoclinic crystal structure with the space group of $P21/c$, which is composed of layers of calcium chloride and dicalcium silicate. Figure 1 shows the XRD patterns of $Ca_3(SiO_4)Cl_2$:Eu^{2+},Mn^{2+}. It can be concluded that the as-synthesized samples are generally of a single phase that is consistent with the low-temperature phase $Ca_3SiO_4Cl_2$ (JCPDS: 24–0032). The substitution of europium and manganese ions does not induce any significant phase change.

Figure 2 shows the powder diffuse reflection spectra of the host, Eu^{2+} singly doped, and Eu^{2+} and Mn^{2+} codoped samples. It is obvious that the host $Ca_3(SiO_4)Cl_2$ shows a platform of high reflection in the wavelength range of 350–800 nm and then starts to decrease dramatically from 350 to 200 nm, due to the host absorption. From curve 1, the low-energy edge of the host absorption can be estimated at around 5.4 eV. When the Eu^{2+} ion is singly doped into the host, two broad bands appear between 250 and 500 nm, which are derived from the 4f–5d electronic dipole allowed transitions of Eu^{2+} ion with the electronic configuration of $4f^65d$. For $Ca_3(SiO_4)Cl_2$:Eu^{2+},Mn^{2+}, a similar spectrum is observed, except for the enhanced absorption intensity. Mn^{2+} ions may also contribute to the increased absorption intensity in the wavelength range from 250 to 550 nm by means of the metal–ligand charge transfer band of Mn^{2+}–O^{2-} and 3d–3d forbidden transitions of Mn^{2+} ion with the electronic configuration of $3d^5$.[17]

Figure 3 shows the excitation and emission spectra of $Ca_3(SiO_4)Cl_2$:0.09Eu^{2+},xMn^{2+} (x = 0, 0.06, 0.09, 0.12, 0.15, 0.18). For x = 0, $Ca_3(SiO_4)Cl_2$:0.09Eu^{2+} shows an intense green broad-band emission around 509 nm upon 395 nm excitation, due to the electric dipole allowed transition of Eu^{2+} ion from the lowest level of the 5d excited state to the 4f ground state, and its full width at half maximum is about 2440 cm^{-1}. Monitoring the green emission at 509 nm, there are several broad bands around 275, 323, 368, and 454 nm. The fine structure of the excitation spectra of Eu^{2+} ion indicates that the site occupied by the Eu^{2+} ion has a lower symmetry. The redshift of the Eu^{2+} ion expressed by the depression value of the lowest excited 5d level in the present host when compared to the free gaseous ion is calculated to be 14,350 cm^{-1}. The Stokes shift is about 2380 cm^{-1}. These results are in general agreement with those reported by Liu and Wanmaker.[15,18]

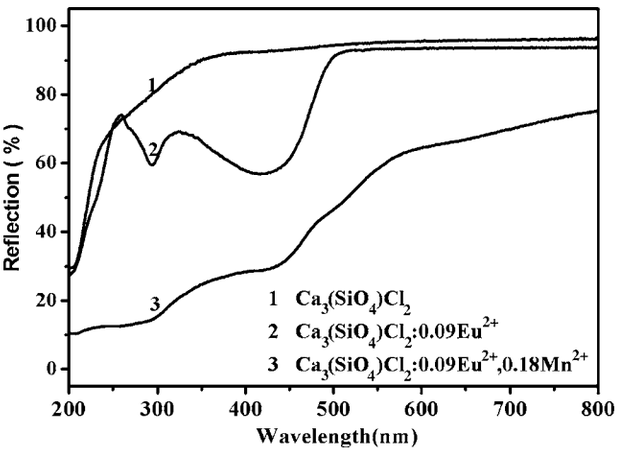

Figure 2. Powder diffuse reflection spectra of $Ca_3(SiO_4)Cl_2$, $Ca_3(SiO_4)Cl_2$:0.09Eu^{2+}, and $Ca_3(SiO_4)Cl_2$:0.09Eu^{2+},0.18Mn^{2+}.

For x = 0.06–0.18, the $Ca_3(SiO_4)Cl_2$:0.09Eu^{2+},xMn^{2+} samples show an additional strong yellow broad-band emission around 568 nm besides the green one. The new yellow emission band is considered to be associated with the Mn^{2+} ion. For this purpose, the sample $Ca_3(SiO_4)Cl_2$:0.09Mn^{2+} was also synthesized and optically investigated. It shows a much lower optical property of the Mn^{2+} ion. For clarity, the emission slit was set at 5 nm for $Ca_3SiO_4Cl_2$:Mn but at 1 nm for $Ca_3SiO_4Cl_2$:Eu,Mn when the signals were recorded. Figure 4 shows several broad bands and peaks in the wavelength range of 300–500 nm, due to the transitions of the Mn^{2+} ion from the ground state $^6A_{1g}(^6S)$ to the crystal field components of the excited $^4E_g(^4D)$, $^4T_{2g}(^4D)$, ^4E_g–$^4A_{1g}(^4G)$, $^4T_{2g}(^4G)$, and $^4T_{1g}(^4G)$ levels.[18] Under excitation at 419 nm, one broad emission band is predominant around 570 nm, assigned to the transition of the Mn^{2+}

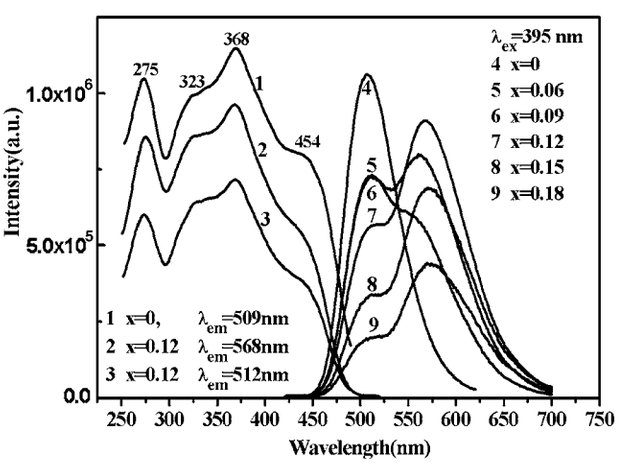

Figure 3. The excitation and emission spectra of $Ca_3(SiO_4)Cl_2$:0.09Eu^{2+},xMn^{2+} (x = 0, 0.06, 0.09, 0.12, 0.15, 0.18).

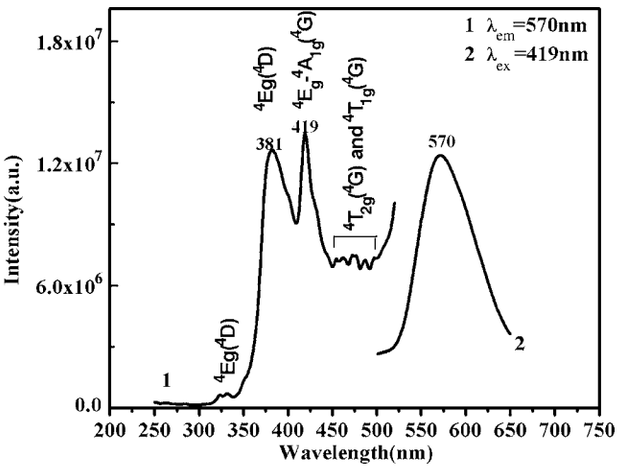

Figure 4. The excitation and emission spectra of $Ca_3(SiO_4)Cl_2$:0.09Mn^{2+}.

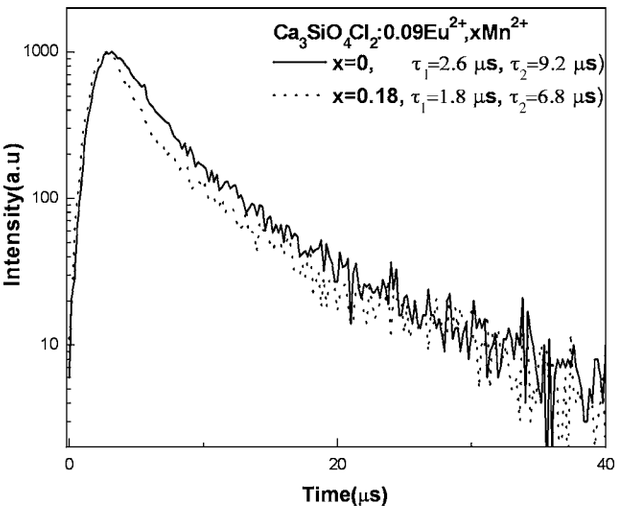

Figure 5. The decay curves of Eu^{2+} ion in $Ca_3(SiO_4)Cl_2$:0.09Eu^{2+},$x$$Mn^{2+}$ (x = 0 and 0.18).

ion from the lowest excited level of $^4T_{1g}(^4G)$ to the ground state $^6A_{1g}(^6S)$. Consequently, a new yellow emission band in Eu^{2+},Mn^{2+} codoped samples is derived from the Mn^{2+} ion. The Mn^{2+} ion in solid compounds is usually characterized by green or orange–red emissions. The emission color is strongly dependent on the coordination environment of the Mn^{2+} ion in the host lattice, such as the strength of the ligand field and coordination number (CN). The stronger the ligand field, the longer the emission peak will be.[19] The CN also has a huge effect on the emission color: the Mn^{2+} ion emits green light when it is tetrahedrally coordinated (CN = 4) in the lattice, whereas it emits orange–red light in an octahedral coordination (CN = 6).[20] For example, the Mn^{2+} ion substitutes the cation site with tetrahedral symmetry in Zn_2SiO_4 and emits intense green light around 520 nm, whereas it occupies the Zn site with octahedral coordination in $Zn_3(PO_4)_2$ and emits red light at 616 nm.[17,21] In the present case, the broad emission band around 568 nm indicates that the Mn^{2+} ion occupies an octahedral site.

Monitoring the yellow emission at 568 nm, the Mn^{2+} ion shows the same excitation features as the Eu^{2+} ion, as shown in curves 2 and 3 of Fig. 3. Here, the 3d–3d forbidden transition bands of the Mn^{2+} ion with low oscillator strength are so weak as to be hidden behind the 4f–5d allowed transition band of the Eu^{2+} ion with a high oscillator strength. The effect of the Mn^{2+} ion concentration was also studied. As shown in Fig. 3, the yellow emission intensity enhances, whereas the green one decreases gradually when the concentration of the Mn^{2+} ion increases. These results support the efficient energy transfer from Eu^{2+} to Mn^{2+} ions.[22,23] The emission intensity of the Mn^{2+} ion attains the maximum at x = 0.12 and then starts to decrease due to the concentration quenching of the Mn^{2+} ion.

The PL decay curves of Eu^{2+} in $Ca_3(SiO_4)Cl_2$:0.09Eu^{2+},$x$$Mn^{2+}$ (x = 0, 0.06, 0.09, 0.12, 0.15, 0.18) were measured and are presented in Fig. 5 and 6. All the decay curves can be well fitted by the double-exponential equation given by

$$I(t) = I_0 + Ae^{-t/\tau_1} + Be^{-t/\tau_2} \quad [1]$$

where I_0 and I are the luminescence intensities at time 0; t, A, and B are constants; τ_1 and τ_2 are the lifetimes for the exponential components, respectively.[6] For $Ca_3(SiO_4)Cl_2$:0.09Eu^{2+}, the lifetimes are determined to be 2.6 and 9.2 μs. These results indicate that there are two lattice sites occupied by Eu^{2+} ions, which is also supported by the emission spectra of $Ca_3(SiO_4)Cl_2$:Eu^{2+}. As shown in Fig. 3, the $Ca_3(SiO_4)Cl_2$:Eu^{2+} phosphor shows an asymmetrical emission band at 508 nm, tailing toward 600 nm, suggesting that two strongly overlapping emission bands exist. The lifetime of the Eu^{2+} ion is usually in the range of 0.2–2 μs.[24-26] However, it is beyond the normal range in a few host compounds. For example, in $BaSi_2O_5$:Eu^{2+} and $Ba_2Mg(BO_3)_2$:Eu^{2+} host lattices, relatively long decay times are 3.3 and 12.6 μs, respectively.[27] Poort et al. state that such an anomalous lifetime is due to a larger delocalization in the excited state where the wave function overlap between the electron and the hole will be largely reduced, resulting in a longer lifetime. In our case, the Eu^{2+} ions may also experience a similar condition. When Mn^{2+} ions are doped into $Ca_3(SiO_4)Cl_2$:0.09Eu^{2+}, the decay lifetimes for Eu^{2+} ion are found to generally decrease with increasing the Mn^{2+} ion concentration, as shown in Fig. 6. For $Ca_3(SiO_4)Cl_2$:0.09Eu^{2+},0.18Mn^{2+}, the decay lifetimes for the Eu^{2+} ion are 1.8 and 6.8 μs. These results are reasonable for the 5d–4f allowed transition of Eu^{2+} ions of less than microseconds.[27] The trend in lifetime for the Eu^{2+} ion in the absence and presence of the Mn^{2+} ion provides strong evidence for energy transfer from Eu^{2+} to Mn^{2+}.[23]

The energy transfer efficiency (η_T) from Eu^{2+} to Mn^{2+} was evaluated based on the following expression[28]

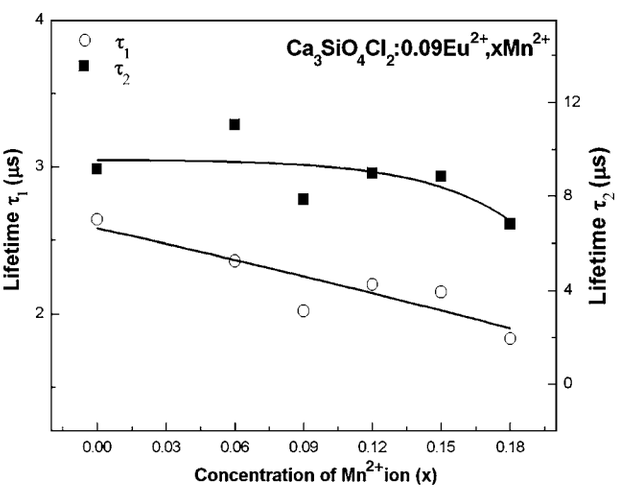

Figure 6. Dependence of the lifetime of Eu^{2+} ion on $Ca_3(SiO_4)Cl_2$:0.09Eu^{2+},$x$$Mn^{2+}$ on Mn^{2+} content x.

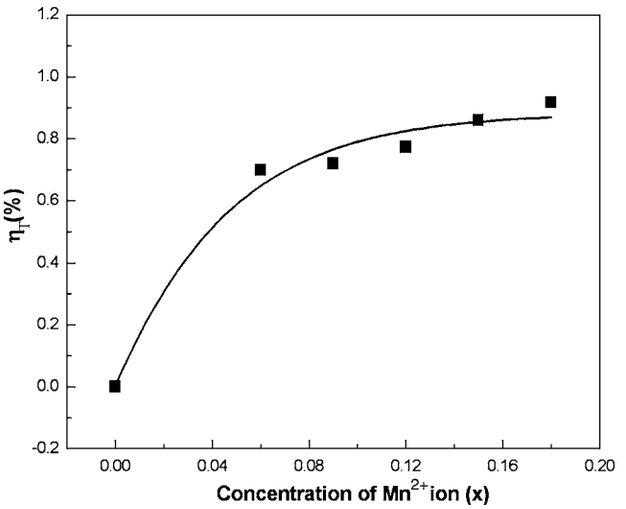

Figure 7. Dependence of the energy transfer efficiency η_T in $Ca_3(SiO_4)Cl_2$:0.09Eu^{2+},xMn^{2+}.

$$\eta_T = 1 - I_d/I_{d0} \quad [2]$$

where η_T is energy transfer efficiency, I_{d0} and I_d are the corresponding intensities of the donor Eu^{2+} ion in the absence and presence of the acceptor Mn^{2+}. As Fig. 7 shows, the energy transfer efficiency η_T is found to increase gradually with increasing Mn^{2+} dopant content and finally saturate, which is similar to $Ce^{3+} \rightarrow Eu^{2+}$ in Ba_2ZnS_3.[22]

The excitation and emission spectra suggest that the phosphors $Ca_3SiO_4Cl_2$:0.09Eu^{2+},xMn^{2+} are a series of efficient dual-chromatic emitting phosphors with broad absorption bands, matching well with the widely used near-UV LED chips (380–420 nm). Figure 8 shows the CIE 1931 chromaticity diagram of the phosphors $Ca_3SiO_4Cl_2$:0.09Eu^{2+},xMn^{2+}. The UV excitation light is selected at

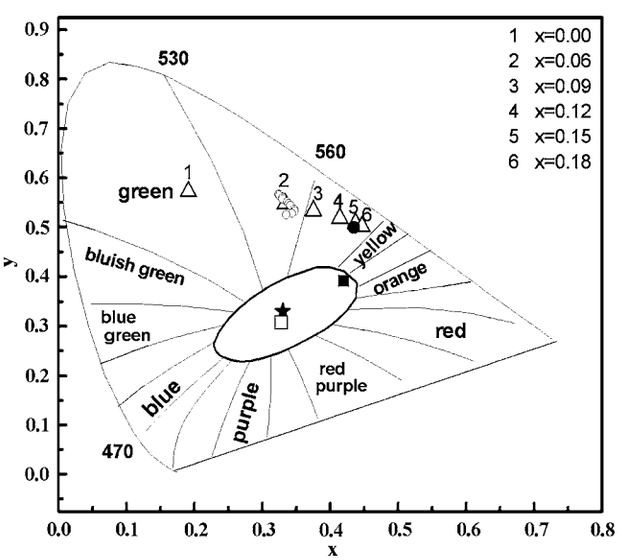

Figure 8. The CIE 1931 chromaticity diagram of $Ca_3SiO_4Cl_2$:0.09Eu^{2+},xMn^{2+} (△, $x = 0$, 0.06, 0.09, 0.12, 0.15, 0.18), $Ca_3SiO_4Cl_2$:0.09Eu^{2+},0.06Mn^{2+} with increasing temperature range between 10–450 K (◯), yellow LED (●, n-UVchip + $Ca_3SiO_4Cl_2$:Eu^{2+},Mn^{2+}), white LED (■, n-UV chip + $Ca_3SiO_4Cl_2$:Eu^{2+} with high-temperature phase), white LED (□, n-UV chip + blue chlorophosphate phosphor + $Ca_3SiO_4Cl_2$:Eu^{2+},Mn^{2+}), and the ideal white point (★).

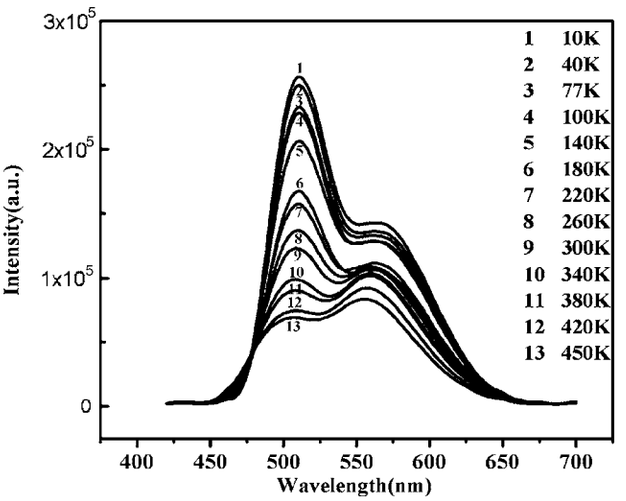

Figure 9. The emission spectra of $Ca_3(SiO_4)Cl_2$:0.09Eu^{2+},0.12Mn^{2+} in range of 10–450 K (λ_{ex} = 395 nm).

395 nm, which is the same as the electroluminescent emission peak of the commercial InGaN chip used in the present case under direct current I_F = 20 mA. The emission light of the Eu^{2+} singly doped phosphor with the color coordination of (0.191,0.572) is situated in the green area. For $Ca_3SiO_4Cl_2$:0.09Eu^{2+},0.18Mn^{2+}, the color coordination is (0.447,0.501) in the yellow region. Along the line between the two end points, the emission color is tunable in the visible region from green to yellow by controlling the concentration of the Mn^{2+} ions. Therefore, the series $Ca_3SiO_4Cl_2$:Eu^{2+},Mn^{2+} are promising candidates for color tunable phosphors of the n-UV pc-wLEDs.

The temperature dependence of the emission characteristics of $Ca_3(SiO_4)Cl_2$:Eu^{2+},Mn^{2+} was investigated in the temperature range of 10–450 K, as shown in Fig. 9 and 10. The intensities of both the green and yellow emissions decrease with increasing temperature. The emission intensity of the Eu^{2+} ion is thermally quenched at a lower temperature than that of Mn^{2+} ion: the quenching temperature, at which the initial PL intensity at 10 K is halved, is 250 K for the Eu^{2+} ion and above 450 K for the Mn^{2+} ion. The decrease in emission intensity with increasing temperature is due to the temperature dependence of the electron–phonon interaction in both the ground state and excited states of the luminescence center.[29] This nonradi-

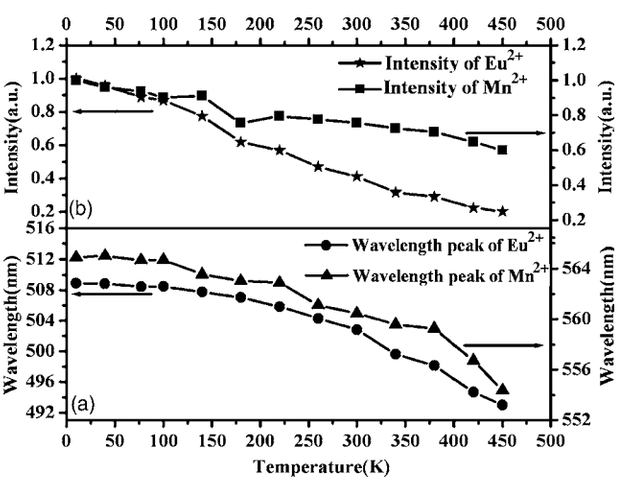

Figure 10. (a) The emission blueshift and (b) thermal quenching curve of $Ca_3(SiO_4)Cl_2$:0.09Eu^{2+},0.12Mn^{2+}.

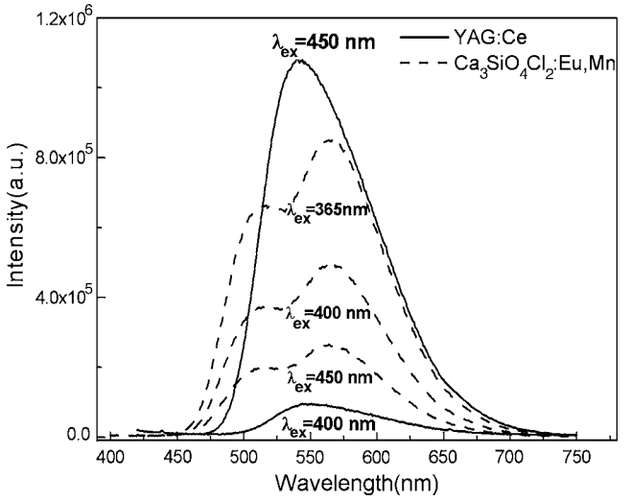

Figure 11. Comparison of the emission spectra of $Ca_3(SiO_4)Cl_2$:0.09Eu^{2+},0.12Mn^{2+} and YAG:Ce.

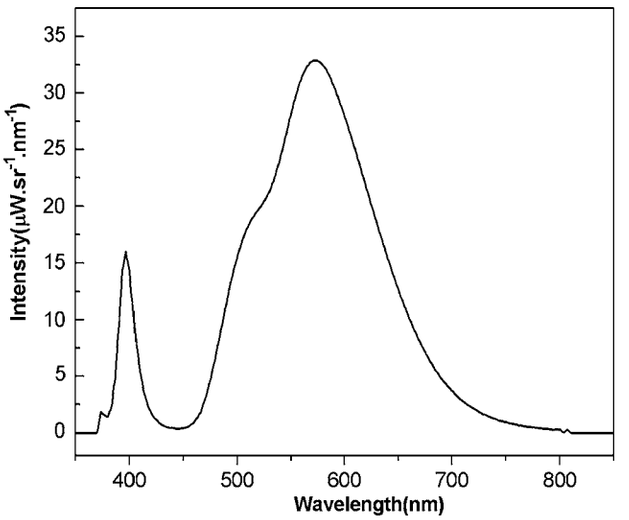

Figure 12. The electroluminescence spectra of the yellow LED based on $Ca_3SiO_4Cl_2$:Eu^{2+},Mn^{2+} under I_F = 20 mA.

ative transition probability by thermal activation is strongly dependent on temperature, resulting in the decrease of the emission intensity. Comparatively, a high quenching temperature for the Mn^{2+} ion indicates a weaker electron–phonon interaction or higher thermal activation energy in the present case. Typically, the emission peak shifts to a lower energy as the temperature is increased.[30] However, the peak positions of the emission spectra are blueshifted with increasing temperature in our case: the peak positions of Eu^{2+} ion at 10 and 450 K are 509 and 493 nm, and those of Mn^{2+} ion at 10 and 450 K are 565 and 554 nm. The same phenomenon was also observed in M_2SiO_4:Eu^{2+} (M = Ca and Ba) where there are two different sites, M(1) and M(2).[31] In Ca_2SiO_4:Eu^{2+}, the single asymmetrical emission at 514 nm is dominant, and in Ba_2SiO_4:Eu^{2+}, the single asymmetrical emission at 507 nm dominates. Both of them exhibit an unusual blueshift with increasing temperature. To account for this phenomenon, the authors proposed that a thermally active phonon-assisted tunneling from the excited states of the low-energy emission band [M(2)] to the excited states of the high-energy emission band [M(1)] in the configuration coordinate diagram occurred. In our case, the Eu^{2+} ion shows an asymmetrical emission band and two lifetimes as shown in Fig. 3, 5, and 6. As discussed above, these results indicate that there are two distinct lattice sites, Eu_I and Eu_{II}, in $Ca_3(SiO_4)Cl_2$. Therefore, a similar tunneling process may also occur between the excited states of Eu_I and Eu_{II} as the temperature increases.

The color stability of phosphor against temperature is a significant factor for a high-power LED device, the joint temperature of which is generally around 420 K. Figure 8 also shows the CIE 1931 chromaticity diagram of $Ca_3(SiO_4)Cl_2$:0.09Eu^{2+},0.06Mn^{2+} with increasing temperature. With the temperature increasing, the *x* value increases from 0.324 (10 K) to 0.348 (380 K) and then decreases to 0.335 (450 K), whereas the *y* value gradually decreases from 0.566 (10 K) to 0.525 (450 K). The slight variation of color coordinates is due to different thermal quenching behaviors and the blueshift of the green and yellow emission of $Ca_3(SiO_4)Cl_2$:Eu^{2+},Mn^{2+} in the temperature range 10–450 K. These results show that the as-synthesized phosphors have a good color stability, especially at a joint temperature from 340 to 450 K.

In order to demonstrate the potential application in white LED, the performance of the yellow phosphor $Ca_3(SiO_4)Cl_2$:0.09Eu^{2+},0.12Mn^{2+} is compared against a home-prepared yttrium aluminum garnet phosphor (YAG:Ce) as shown in Fig. 11. The excitation wavelength is chosen at 400 and 450 nm because they are well matched with the dominating emission band of the commercial blue and UV LED chips. It is estimated that the integrated emission intensity of $Ca_3SiO_4Cl_2$:Eu,Mn is 5.5 times as intense as that of home-prepared YAG:Ce when the excitation wavelength is at 400 nm. And, the integrated emission intensity of home-prepared YAG:Ce is 3.5 times as strong as that of $Ca_3SiO_4Cl_2$:Eu,Mn when the excitation wavelength is at 450 nm. In addition, it is estimated that the performance (λ_{ex} = 365 nm) of $Ca_3SiO_4Cl_2$:Eu,Mn reaches 96% of home-prepared YAG:Ce (λ_{ex} = 450 nm). These results indicate that $Ca_3SiO_4Cl_2$:Eu,Mn is ideal for 365 or 400 nm UV LED applications. Because of the scarcity of the 365 nm UV chip, the 400 nm UV chip was chosen to fabricate the phosphor converted white LED.

Yellow and white LED application of $Ca_3SiO_4Cl_2$:Eu^{2+}–Mn^{2+}.— Figure 12 shows the intense yellow LED fabricated with the $Ca_3SiO_4Cl_2$:Eu^{2+},Mn^{2+} under I_F = 20 mA. It is obvious that there are three emission bands: the weak sharp band at 395 nm, the dominant band at 570 nm, and the intense shoulder around 510 nm, respectively. The UV emission is due to the electroluminescence of the UV GaN chip. The green and yellow emissions are consistent with the PL emission spectra of $Ca_3SiO_4Cl_2$:Eu^{2+},Mn^{2+} as shown in Fig. 3. The fabricated LED shows a much lower UV light intensity, indicating this $Ca_3SiO_4Cl_2$:Eu^{2+},Mn^{2+} phosphor has a high UV absorption efficiency and high down-converting efficiency. It is essential for the white LEDs fabricated with the near-UV chip and phosphors to prevent the UV light from leaking out because the UV light is harmful to human eyes and degrades the packing resins. The color coordinate of the as-fabricated LED is (0.4348, 0.4985) as shown in Fig. 8 (●) under I_F = 20 mA.

Liu et al. reported the white LED based on the n-UV (E_m = 402 nm) InGaN chip and a monochromatic emitting phosphor $Ca_3SiO_4Cl_2$:Eu^{2+} with the high-temperature phase. The white light of such a w-LED is located at the edge of the white circle near the yellow region (■, in Fig. 8) and only has a color-rendering index of 73 because of the lack of blue and green content in the white emission.[13] In our case, the white LED with the improved chromaticity quality was successfully fabricated by combining the UV chip and blue chlorophosphate and green/yellow chlorosilicate phosphors. As shown in Fig. 13, the emission bands are located at about 397, 454, 510, and 570 nm, derived from the n-UV LED and the blue and green/yellow phosphors, respectively. The color coordinate and correlated-color temperature T_c of the two-phosphor white LED are about (0.3281, 0.3071) and 6065 K, respectively. The luminous efficiency (η_L) and the color-rendering index R_a are 11 lm/W and

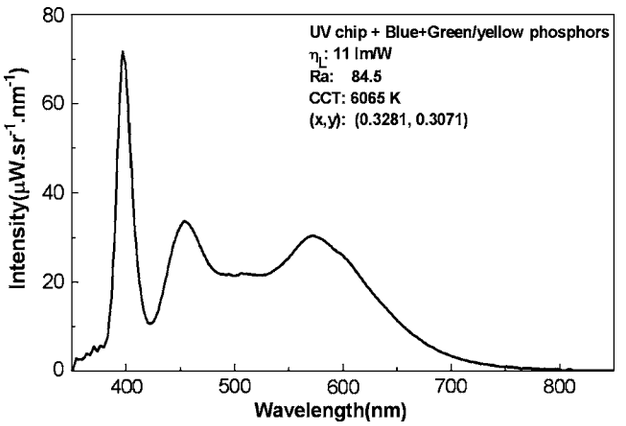

Figure 13. The electroluminescence spectra of the white LEDs based on UV chips, the blend of blue chlorophosphate and green/yellow $Ca_3SiO_4Cl_2:Eu^{2+},Mn^{2+}$ phosphors.

84.5, higher than those (η_L = 3.8, 6, or 9 lm/W; R_a = 68, 85, or 78) fabricated with a UV chip and strontium silicate or calcium pyrophosphates phosphor.[32-34] The two-phosphor white LED based on a UV chip also shows a higher R_a than the commercial white LED ($R_a \approx 75$) based on the blue chip and yellow YAG:Ce phosphor.

Conclusion

In summary, a series of intense yellow phosphors, $Ca_3SiO_4Cl_2:Eu^{2+},Mn^{2+}$, is reported. They exhibit the efficient broad absorption band, intense green to yellow tunable emission, high efficient energy transfer between Eu^{2+} and Mn^{2+}, and good color stability with increasing temperature. The yellow LED based on $Ca_3SiO_4Cl_2:Eu^{2+},Mn^{2+}$ shows the intense yellow light and much lower UV light leakage. The white LED based on the UV chip, blue phosphor, and $Ca_3SiO_4Cl_2:Eu^{2+},Mn^{2+}$ produces good white light [(0.3281, 0.3071), 6065 K, 84.5, and 11 lm/W]. These results indicate that $Ca_3SiO_4Cl_2:Eu^{2+},Mn^{2+}$ is a promising phosphor applicable to near-UV LEDs for solid-state lighting.

Acknowledgments

We acknowledge financial support from the National Natural Science Foundation of China (20501023), the Nature Science Foundation of Guangdong Province (5300527), and the Science and Technology Project of Guangzhou (2005Z2-D0061).

References

1. S. Nakamura, M. Senoh, and T. Mukai, *Appl. Phys. Lett.*, **62**, 2390 (1993).
2. Y. Uchida and T. Tagchi, *Opt. Eng.*, **44**, 124003 (2005).
3. J. K. Sheu, S. J. Chang, C. H. Ku, Y. K. Su, L. W. Wu, Y. C. Lin, W. C. Lai, J. M. Tsai, G. C. Chi, and R. K. Wu, *IEEE Photon. Technol. Lett.*, **15**, 18 (2003).
4. J. K. Park, C. H. Kim, S. H. Park, and H. D. Park, *Appl. Phys. Lett.*, **84**, 1647 (2004).
5. E. Radkov, R. Bompiedi, A. M. Srivastava, A. A. Setlur, and C. Becker, *Proc. SPIE*, **5187**, 171 (2004).
6. M. Zhang, J. Wang, W. J. Ding, Q. H. Zhang, and Q. Su, *Appl. Phys. B: Lasers Opt.*, **86**, 647 (2007).
7. Y. Q. Li, G. de With, and H. T. Hintzen, *J. Mater. Chem.*, **15**, 4492 (2005).
8. W. J. Ding, J. Wang, M. Zhang, Q. H. Zhang, and Q. Su, *Chem. Phys. Lett.*, **435**, 301 (2007).
9. R.-J. Xie, N. Hirosaki, M. Mitomo, K. Takahashi, and K. Sakuma, *Appl. Phys. Lett.*, **88**, 101104 (2006).
10. H. A. Hoppe, F. Stadler, O. Oeckler, and W. Schnick, *Angew. Chem. Int. Ed.*, **43**, 5540 (2004).
11. K. Uheda, N. Hirosaki, Y. Yamamoto, A. Naito, T. Nakajima, and H. Yamamoto, *Electrochem. Solid-State Lett.*, **9**, H22 (2006).
12. Q. H. Zeng, H. Tanno, K. Egoshi, N. Tanamachi, and S. X. Zhang, *Appl. Phys. Lett.*, **88**, 051906 (2006).
13. J. Liu, H. Z. Lian, C. S. Shi, and J. Y. Sun, *J. Electrochem. Soc.*, **152**, G880 (2005).
14. W. J. Ding, J. Wang, M. Zhang, Q. H. Zhang, and Q. Su, *J. Solid State Chem.*, **179**, 3582 (2006).
15. J. Liu, H. Z. Lian, J. Y. Sun, and C. S. Shi, *Chem. Lett. (Jpn.)*, **34**, 1340 (2005).
16. Y. X. Pan, M. M. Wu, and Q. Su, *J. Phys. Chem. Solids*, **65**, 845 (2004).
17. J. Wang, S. B. Wang, and Q. Su, *J. Mater. Chem.*, **14**, 2569 (2004).
18. W. L. Wanmaker, J. W. Ter Vruggt, and A. Bril, *Philips Res. Rep.*, **23**, 189 (1968).
19. S. Parke, *J. Phys. Chem. Solids*, **32**, 669 (1971).
20. S. Linwood and J. Wegl, *J. Opt. Soc. Am.*, **42**, 910 (1952).
21. L. M. Xiong, J. L. Shi, J. L. Gu, L. Li, W. M. Huang, J. H. Gao, and M. L. Ruan, *J. Phys. Chem. B*, **109**, 731 (2005).
22. W. J. Yang and T. M. Chen, *Appl. Phys. Lett.*, **90**, 171908 (2007).
23. W. J. Yang, L. Y. Luo, T. M. Chen, and N. S. Wang, *Chem. Mater.*, **17**, 3883 (2005).
24. J. L. Sommerdijk, J. M. P. J. Verstegen, and A. Bril, *J. Lumin.*, **8**, 502 (1974).
25. R. F. Sosa, E. R. Alvarez, M. A. Comacho, A. F. Munoz, and J. O. Rubio, *J. Phys.: Condens. Matter*, **7**, 6561 (1995).
26. G. Blasse, W. L. Wanmaker, J. W. Ter Vruggt, and A. Bril, *Philips Res. Rep.*, **23**, 189 (1968).
27. S. H. M. Poort, A. Meijerink, and G. Blasse, *J. Phys. Chem. Solids*, **58**, 1451 (1997).
28. P. I. Paulose, G. Jose, V. Thomas, N. V. Unnikrishnan, and M. K. R. Warrier, *J. Phys. Chem. Solids*, **64**, 841 (2003).
29. V. B. Mikhailikm, H. Kraus, D. Wahl, M. Itoh, M. Koike, and I. K. Bailiff, *Phys. Rev. B*, **69**, 20510 (2004).
30. D. Hsu and J. L. Skinner, *J. Chem. Phys.*, **81**, 5471 (1984).
31. J. S. Kim, Y. H. Park, S. M. Kim, J. C. Choi, and H. L. Park, *Solid State Commun.*, **133**, 445 (2005).
32. J. K. Park, M. A. Lim, C. H. Kim, H. D. Park, J. T. Park, and S. Y. Choi, *Appl. Phys. Lett.*, **82**, 683 (2003).
33. X. Y. Sun, J. H. Zhang, X. Zhang, S. Z. Lu, and X. J. Wang, *J. Lumin.*, **122–123**, 955 (2007).
34. Z. D. Hao, J. H. Zhang, X. Zhang, X. Y. Sun, Y. S. Luo, S. Z. Lu, and X. J. Wang, *Appl. Phys. Lett.*, **90**, 261113 (2007).